Technical Sciences
Academy of Romania
www.jesi.astr.ro

Journal of Engineering Sciences and Innovation
Volume 8, Issue 4 / 2023, pp. 347-362

A. Mechanical Engineering

Received ***27 June 2023*** *Accepted* ***4 December 2023***
Received in revised form ***6 October 2023***

Design and kinematic modeling of a mobile manipulator with hybrid locomotion for agricultural applications

IOAN DOROFTEI[1,2*], CLAUDIA–ANA MORAR[1], MARIUS–GHEORGHE HAGAN[1]

[1]*„Gheorghe Asachi" Technical University of Iasi, 43 D. Mangeron Blvd, 700050, Iasi, Romania*
[2]*Technical Sciences Academy of Romania, 26 Dacia Blvd, 030167, Bucharest, Romania*

Abstract. In agriculture, one of the future solutions to eliminate the negative effect on the environment of the classical machineries is to use mobile robots. Small groups of mobile robots will interact with each other in order to inspect, to process or to harvest crops. These robots will have to work in a changing environment, in terms of terrain or road surfaces, the light of the ambient, animals, etc., aspects that will pose challenges for mobile robots. To facilitate the use of robots in agriculture, they must have a simple construction, be extremely reliable, flexible and, last but not least, cheap. These aspects have as effect new challenges for robot manufacturers to find technical solutions to meet the mentioned requirements. In this paper, a conceptual design and modeling of a mobile manipulator with hybrid locomotion, which may be used in agriculture for applications, such as tilling, seeding, weeding, etc, will be discussed.

Keywords: mobile manipulator, hybrid locomotion, agricultural applications

1. Introduction

One of the future solutions to eliminate the negative effect on the environment of classic agricultural machines is the use of mobile robots in agriculture. These robots will have to operate in a constantly changing environment (terrain, roads, ambient lighting, biological objects, etc.). To enable robotics to enter the agricultural sector, the robots must have a simple construction, be highly reliable, flexible and, last but not least, cheap.
Despite the advantages (among them, minimizing pollution, maximizing production, replacing human labor with robots, etc.), there are also significant

*Correspondence address: idorofte@mail.tuiasi.ro

challenges: the complexity of the agricultural environment (complex and variable environments, diverse terrains, obstacles, fluctuating weather conditions); precise navigation and localization (agricultural robots must move precisely in the field and locate themselves correctly); delicate handling of crops (agricultural crops can be delicate and sensitive to improper handling); interaction with the natural environment (agricultural robots must interact effectively and safely with the natural environment, including plants, soil and animals); costs and profitability (implementing agricultural robots can be expensive).

The purpose of this paper is to present a laboratory concept for a mobile manipulator with hybrid locomotion that could be, on a large scale, used for some agricultural applications (plant inspection, weeding, their chemical treatment or soil loosening, etc.).

The paper is organized as follows: first some agricultural robots, by application category, are presented; then the locomotion systems used for these robots are discused; section 4 presents the design of a proposed agricultural robot with hybrid locomotion and its mathematical modeling; conclusions are given in section 5.

2. Agricultural robots, by application category

According to a study done by Oliveira, L.F.P. et al., 2021 [1], most agricultural robots are encountered in weeding or grape picking applications (Fig. 1).

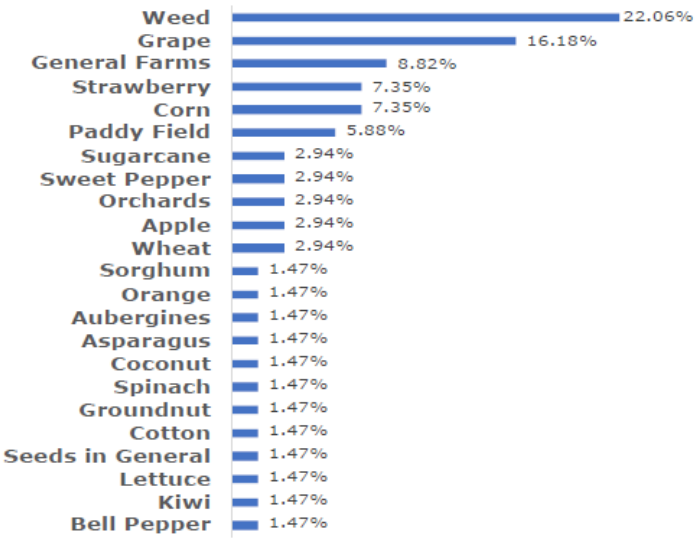

Fig. 1. Agricultural robot by application category [1].

The different agricultural activities that can be performed by robots can be grouped into the following application categories [1]: land preparation before planting (Fig. 2); sowing/planting (Fig. 3); plant treatment (Fig. 4); harvesting (Fig. 5); production estimation and phenotyping (Fig. 6).

(a) (b) (c)

Fig. 2. Examples of robots used in agriculture to prepare the land before planting [1]:
a) the Cäsar robot [2]; b) the Greenbot robot [3]; c) the AgBot robot [4].

(a) (b) (c)

Fig. 3. Examples of robots used in agriculture for sowing and planting [1]:
a) the Lumai-5 robot [5]; b) the Di-Wheel robot [6]; c) Sowing robot 1 [7].

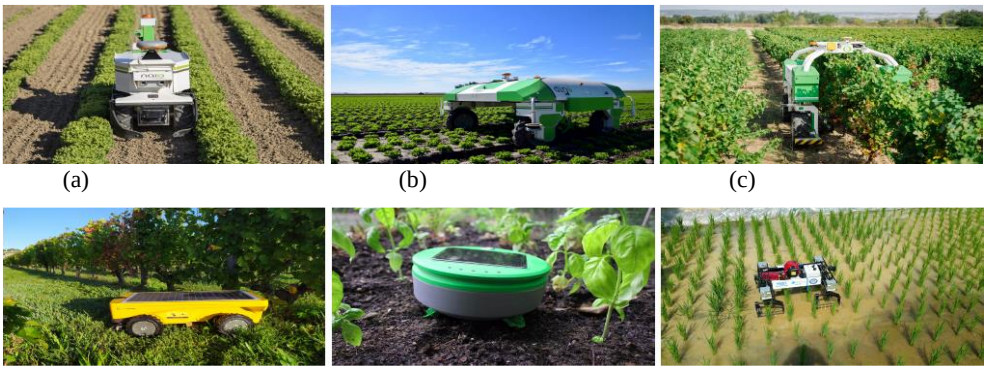

(a) (b) (c)

(d) (e) (f)

Fig. 4. Examples of robots used in agriculture for plant treatment [1]:
a) Oz [8]; b) Dino [9]; c) Ted [10]; d) VITIROBOT [11]; e) Tertill [12]; f) K-Weedbot [13].

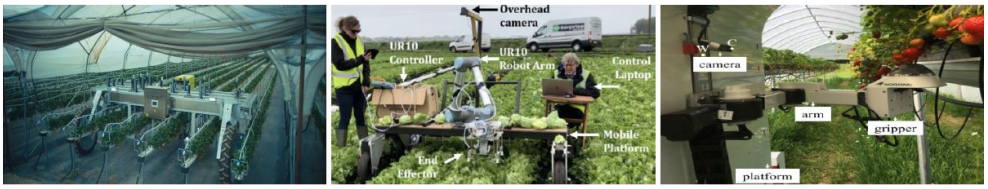

(a) (b) (c)

Fig. 5. Examples of robots used in agriculture for harvesting [1]:
a) Agrobot E-Series [14]; b) Vegebot [15]; c) Noroon [16].

(a) (b) (c)

Fig. 6. Examples of robots used in agriculture for production estimation and phenotyping [1]: a) Shrimp [17]; b) VINBOT [18]; c) VineRobot [19].

3. Locomotion systems used for agricultural robots

The types of locomotion systems found in agricultural robots from the documentation studied by the authors (Oliveira, L.F.P. et al., 2021) are summarized in Fig. 7, where the notations are as following: 4WD – robots with 4 driven wheels; 4WS - robots with 4 driven and stearable wheels; UAV – unmanned flying robots; 2WD – robots with 2 driven wheels; 8WD – robots with 8 driven wheels; 3WD – robots with 3 driven wheels. As can be seen, most mobile platforms with agricultural applications are using wheeled locomotion, 4WD type.

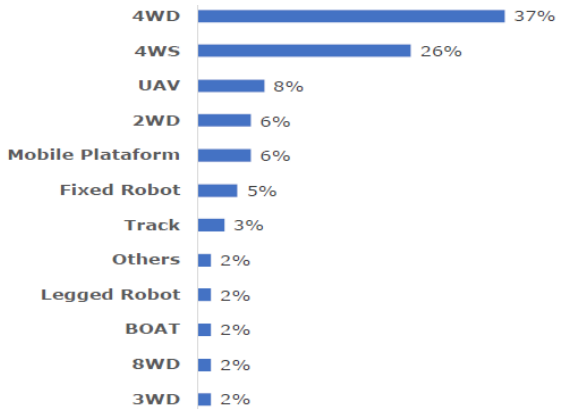

Fig. 7. Locomotion systems for robots used in agriculture [1].

However, wheeled systems are heavily affected by local terrain features such as rocks and branches. In addition, the constant locomotion of these robots throughout the farm results in a high rate of soil compaction. As for UAV systems, improving their flight time can increase their use in agricultural environments. Another alternative for locomotion in unstructured environments is the use of legged robots (these robots have discontinuous contact, they can adjust your posture according to the slope of the terrain, allowing them to navigate rough and hard-to-reach environments). Although they reduce damage to the ground, the legs of conventional walking robots have a small contact area, creating a large pressure on the foot placement region. To prevent robot legs from digging into soft soils and getting stuck, legged robots need to have specially designed foot-to-ground contact areas to reduce pressure.

An alternative to this solution is the use of mobile platforms with hybrid locomotion (wheels and legs). The wheel increases the contact area and allows the vehicle to move at a higher speed when the robot moves outside the work area, for transfer from one greenhouse to another or from one agricultural field to another.

4. Proposed robot design

4.1. Robot specifications and requirements

The type of locomotion of the mobile platform will be chosen taking into account the following criteria: the mobile platform should harm the environment as little as possible; it should be able to move faster during the change of agricultural land/greenhouse; the robot should allow omnidirectional movement; it must move efficiently over terrain (wheels or tracks are less efficient than legs on soft or vegetated terrain); the legs allow more precise positioning of the platform compared to the wheels, sliding less. Based on the previous criteria, the mobile platform will have hybrid locomotion (legs with wheels at their extremities). To simplify the control, the manipulator will have a Cartesian coordinates structure.

4.2. Leg – wheel module design

4.1.1. Structural synthesis of the leg mechanism

The following can be used as starting points for the design of the leg mechanism: the leg structure must be represented by a simple and reliable mechanism; low energy consumption during the stationary mobile platform (while the manipulator performs a certain operation); if possible, in this phase, some leg actuators should not be actuated; the leg must have a minimum number of actuators; as far as possible, the leg should be perpendicular to the ground surface. Among the possible mechanisms, the following mechanisms can be considered: planar Scotch-Yoke mechanism; planar cam mechanism. Both mechanisms could provide the criteria mentioned above, but due to its simpler manufacturing solution, the first mechanism will be adopted.

4.1.2. Leg mechanism kinematics

Typically, a full leg of a walking robot must have three degrees of freedom. For the mobile platform that is to be designed, a leg mechanism with two degrees of freedom is proposed (Fig. 8). Using only two actuators per leg, the trajectory of its extremity in the support phase will be an arc (as consequence, the robot slides a little while walking). But, the main advantage of this kinematics is a minimal resisting torque on the motor in the *B* joint when the leg is on the ground. In order to simplify the mathematical modeling, *B*, *C* and *D* joints will be eliminated, and the rotational kinematic parameter of the *B* joint, θ_2, will be replaced by a

translational kinematic parameter, in the *E* joint (Fig. 8.c), parameter that satisfies the relation:

$$d_4 = l_2 \cdot \cos\theta_2 . \tag{1}$$

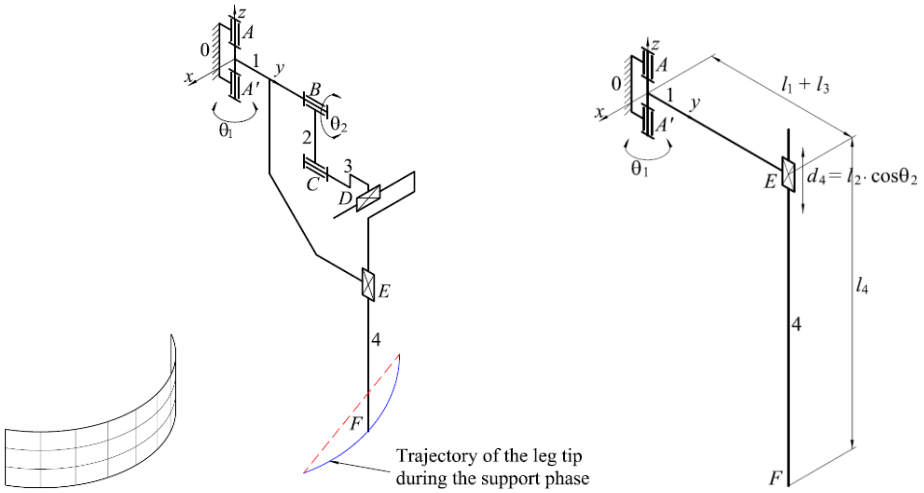

(a) (b) (c)

Fig. 8. Kinematics of the spatial leg mechanism: a) working space of the *F* leg tip; b) trajectory of the leg tip during support phase [20]; c) simplified kinematics of the leg mechanism.

4.1.3. Kinematics of the leg – wheel module mechanism

Mobile robots working on natural terrain must have high maneuverability. Legged vehicles have the ability to adapt better to unstructured terrain, while wheeled platforms can move faster on flat surface. Based on these aspects, hybrid locomotion mobile robots have been designed. One of the possible solutions for such a robot is to use wheels at the end of the leg (Fig. 9). Using this leg solution, the mobile robot can go over the obstacles in a farmland/greenhouse and move faster when it changes farmland/greenhouse.

When the mobile platform moves as a legged vehicle, the wheel will not rotate / steer. This wheel will become active when the mobile robot moves as a wheeled one. To detect the contact with the ground, the *F* prismatic passive joint is used, which allows the closing of an electrical contact between the links *4* and *5*. When this contact closes, the actuator of *B* joint will stop, stopping, in this way, lowering that leg. This allows the robot to maintain its body in a horizontal position when traveling over rough terrain. Returning to the initial position of the link *5* (opening the electrical contact), when the leg rises or loses contact with the ground, is ensured by the helical spring. To correct the lateral displacement of the robot body due using only two actuators per each leg mechanism, when moving the mobile robot using the legs (moving like a walking machine), the wheels at their extremity will be used, in order to correct the trajectory of the *I* leg tip during the support phase (dashed red line in Fig. 9.b).

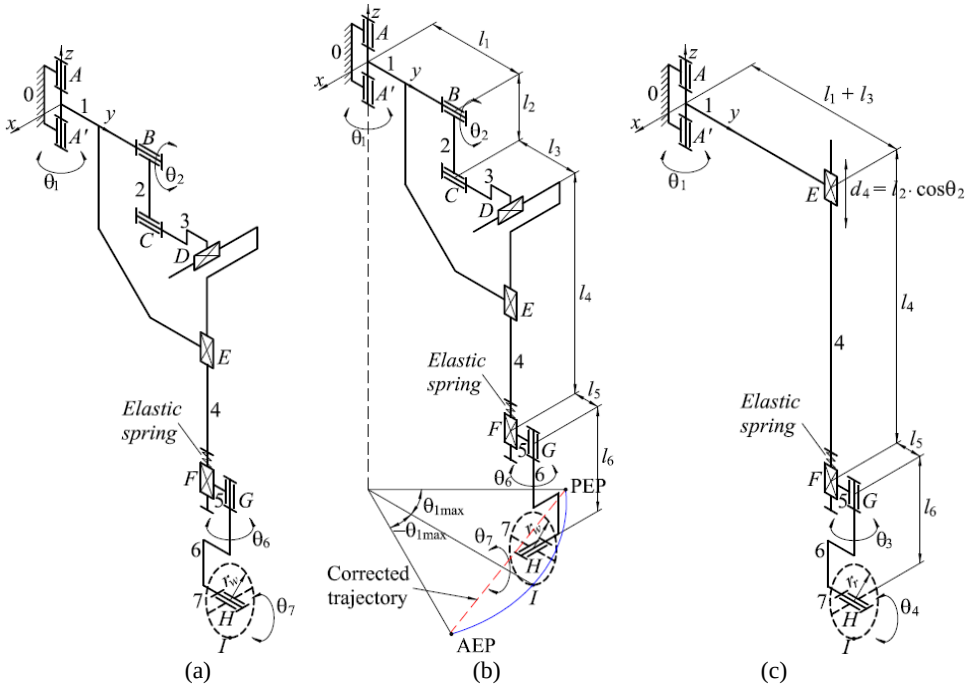

(a) (b) (c)

Fig. 9. Spatial mechanism of the leg-wheel module [20], [21]: a) leg-wheel mechanism in neutral position; b) leg-wheel mechanism with the wheel oriented with $\theta_6 = 90^o$, to correct the trajectory of leg tip *I*; c) simplified kinematics of the leg - wheel mechanism.

Under these conditions, when the mobile manipulator moves like a walking machine, the legs can be considered as having three degrees of mobility (three actuators). In Fig. 9.b, it is considered that the wheel *7* will touch the ground in the Extreme Position Anterior (AEP) of the support phase, when $\theta_1 = -\theta_{1\max}$, and leaves the ground in the Extreme Rear Position of the support phase, when $\theta_1 = \theta_{1\max}$. To correct the circular path colored in blue, the wheel will have to rotate using a variable rotation angle, θ_7, which depends on the value of θ_1:

$$\theta_7 = \frac{180^o}{\pi \cdot r_r} \cdot \left(l_1 + l_3 + l_5\right) \cdot \left[1 - \cos\left(\theta_{1\max} - \theta_1\right)\right], \tag{2}$$

where: r_r is the radius of the wheel; l_1, l_3, l_5 are the lengths of the link 1, 2 and 3. It should be noted that the angular position parameters θ_1 and $\theta_{1\max}$ are positive when the leg rotates clockwise around the axis of the *A* joint, and negative when the leg rotates counterclockwise. For the reasons mentioned above, the leg - wheel mechanism with simplified kinematics, represented in Fig. 9.c, will be used for mathematical modeling.

4.3. Robot design and kinematics

Starting from the leg - wheel mechanism shown in Fig. 9 and the considerations discussed earlier in this paragraph, the overall kinematics of a mobile manipulator for agricultural applications was proposed (Fig. 10). As seen in this figure, a Cartesian coordinate manipulator (Gantry type), the kinematic chain using the *J-J'*, *K*, *L* joints, is mounted on a hybrid locomotion mobile robot.

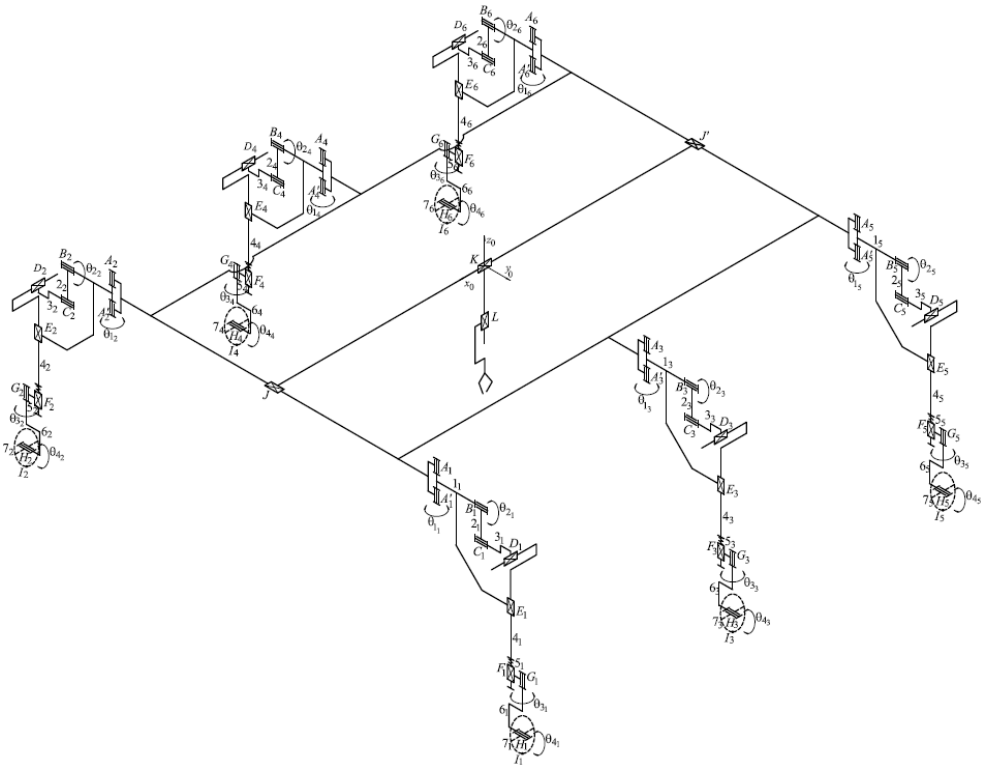

Fig. 10. Kinematics of the proposed mobile manipulator with hybrid locomotion [20], [21].

Due to the use of hybrid locomotion, this mobile manipulator is able to move faster on flat terrain and to instantly change the direction, when acting as a wheeled mobile platform (with 4 or 6 wheels on the ground), or to climb over obstacles and to adapt on unstructured terrain when acting as a mobile platform with legs. The legs also have the role of active suspension. For mathematical modeling, the mobile platform with the simplified leg kinematics (shown in Fig. 9.c) will be used. Based on the kinematics shown in Fig. 10, the 3D CAD model of the hybrid locomotion mobile robot was designed, and a prototype was realized (Fig. 11).

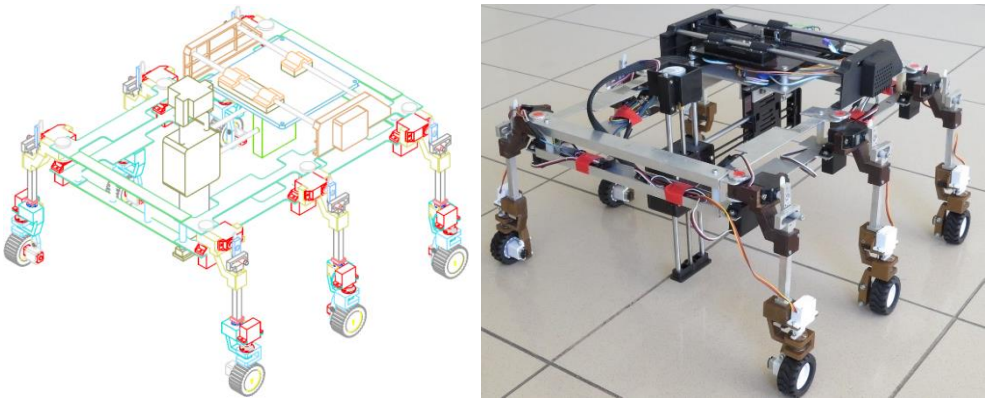

(a) (b)

Fig. 11. Constructive solution of the mobile manipulator [20]: a) 3D CAD design; b) real prototype.

4.4. Possible scenarios of the wheeled locomotion

In its movement using the wheels, the mobile platform can describe a series of trajectories, which will be described in the following.

We consider first the general case of moving the robot along a curved trajectory, with R_R radius (Fig. 12). To avoid sliding, there must be an instantaneous center of rotation, *I*, and the next condition must be respected:

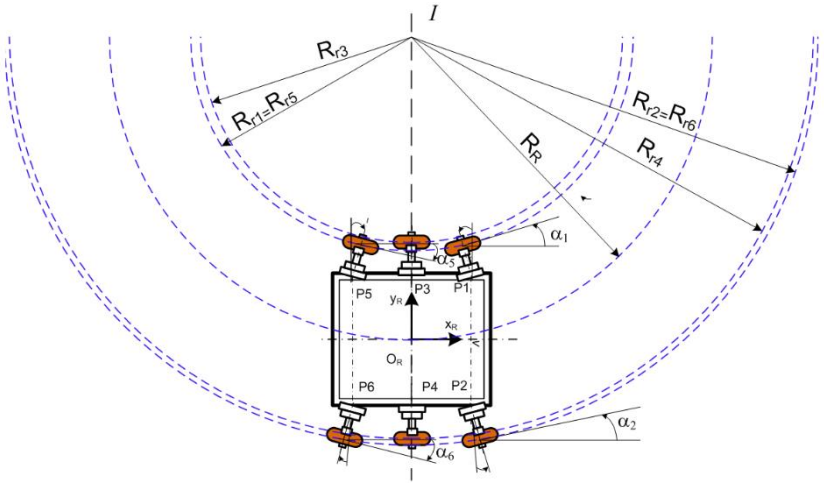

Fig. 12. Mobile robot moving on a curved trajectory with R_R radius.

$$\frac{R_{r1}}{v_2}=\frac{R_{r2}}{v_2}=\frac{R_{r3}}{v_3}=\frac{R_{r4}}{v_4}=\frac{R_{r5}}{v_5}=\frac{R_{r6}}{v_6}=\frac{R_R}{v_R}, \tag{3}$$

where: R_{ri} $(i=1\text{K}\,6)$ are the radii of the trajectories described by the six wheels; v_i denote the peripheral velocities of the wheels; v_R is the speed of the robot

geometrical center. The peripheral velocities of the wheels are calculated using the relation:

$$v_i = \omega_i \cdot r_i, \ \ i = 1\text{K}\ 6, \tag{4}$$

where the angular velocities of the six wheels were denoted by ω_i, and the radii of the wheels by r_i. Theoretically, all the six wheels have the same radius, $r_i = r$. Different values of the wheels radii can occur when the pressure in the tires is not the same, or when the tires have different wear. In the mathematical modeling, these aspects will be neglected. It follows that, for an imposed speed of the robot, v_R, and a radius R_R of its path, the angular velocities of the wheels will be:

$$\omega_i = \frac{v_R \cdot R_{ri}}{v_i \cdot R_R}. \tag{5}$$

If the angular velocities of the wheels are imposed, the linear velocity of the robot will be

$$v_R = \frac{\omega_i \cdot r_i \cdot R_R}{R_{ri}}, \tag{6}$$

and its angular velocity can be determined with the relation

$$\Omega_R = \frac{\omega_i \cdot r_i}{R_{ri}}. \tag{7}$$

The angle between two successive positions of the robot, for a time Δt, will be:

$$\Delta\theta = \Omega_R \cdot \Delta t = \frac{\omega_i \cdot r_i}{R_{ri}} \cdot \Delta t. \tag{8}$$

In order for the axes of the six wheels to meet at the same point (the instantaneous center of rotation), it is necessary that the legs 1, 5, 2 and 6 are oriented with the angles $\alpha_1 = -\alpha_5$ and $\alpha_2 = -\alpha_6$ in relation to the vertical axes passing through the joint (see Fig. 9):

$$|\alpha_1| = \arcsin\left(\frac{L}{R_{r1} + l_1 + l_3 + l_5}\right) = |\alpha_5| = \arcsin\left(\frac{L}{R_{r5} + l_1 + l_3 + l_5}\right), \tag{9}$$

$$|\alpha_2| = \arcsin\left[\frac{L}{R_{r2} - (l_1 + l_3 + l_5)}\right] = |\alpha_6| = \arcsin\left[\frac{L}{R_{r6} - (l_1 + l_3 + l_5)}\right], \tag{10}$$

where *L* is the longitudinal distance between two adjacent legs.
We now consider that the robot pivots around a vertical axis passing through its geometric center (Fig. 13). In this case also there must be an instantaneous center of rotation and the condition (9) must be satisfied. The following relationships are valid for this type of robot movement:

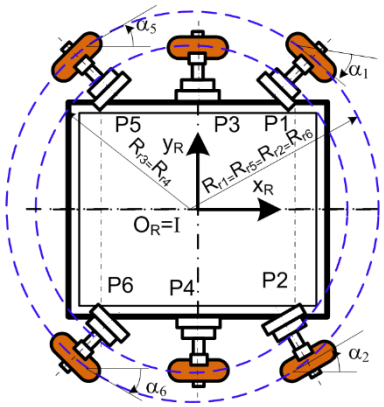

Fig. 13. The wheeled platform pivoting around a vertical axis passing through its geometric center.

$$R_R = 0;\ \ v_R = 0\,, \tag{11}$$

$$\Omega_R = \frac{\omega_i \cdot r_i}{R_{ri}}\,, \tag{12}$$

$$R_{r1} = R_{r5} = R_{r2} = R_{r6};\ \ R_{r3} = R_{r4}\,, \tag{13}$$

$$|\alpha_1| = |\alpha_5| = |\alpha_2| = |\alpha_6| = \arcsin\left[\frac{L}{R_{r1} - (l_1 + l_3 + l_5)}\right]. \tag{14}$$

We assume now that the robot moves along a straight path, in the direction of its longitudinal axis (Fig. 14). All the wheels are, in this case, parallel, the orientation angles of the legs or of the wheels having zero value.

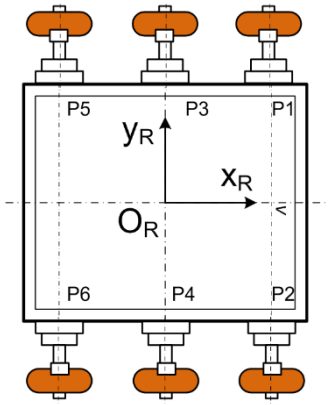

Fig. 14. The wheeled platform moves along a straight path along its longitudinal axis.

The equations that can be written for this type of robot movement are as following:

$$R_R = R_{ri} = \infty;\ \ \Omega_R = \frac{v_R}{R_R} = 0\,, \tag{15}$$

$$\Delta x_R = v_R \cdot \Delta t = v_i \cdot \Delta t = \omega_i \cdot r_i \cdot \Delta t;\ \ i = 1\text{K}\ 6\,, \tag{16}$$

$$\Delta y_R = 0\,, \tag{17}$$

$$\Delta\theta = \Omega_R \cdot \Delta t = \frac{\omega_i \cdot r_i}{R_{ri}} \cdot \Delta t = 0\,. \tag{18}$$

We will now assume that the robot still moves along a straight trajectory, but in a direction different from its longitudinal axis (Fig. 15). In this case also all the wheels are parallel, but their orientation angles are no longer zero. For the orientation of the wheels (with the same angle) the driving motors of the G_i joints are used (see Fig. 9).

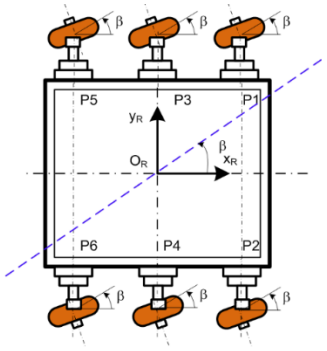

Fig. 15. The wheeled mobile platform translates in a direction different from its longitudinal axis.

The equations (15) and (18) are still valid for this type of robot movement. Also next equations can be written:

$$\Delta x_R = v_R \cdot \Delta t \cdot \cos\beta = v_i \cdot \Delta t \cdot \cos\beta = \omega_i \cdot r_i \cdot \Delta t \cdot \cos\beta;\ \ i = 1\text{K}\ 6\,, \tag{19}$$

$$\Delta y_R = v_R \cdot \Delta t \cdot \sin\beta = v_i \cdot \Delta t \cdot \sin\beta = \omega_i \cdot r_i \cdot \Delta t \cdot \sin\beta;\ \ i = 1\text{K}\ 6\,, \tag{20}$$

4.5. Kinematics of the walking platform

In this paragraph, the forward and inverse kinematics problems of the leg mechanisms will be written, considering the mobile robot as a whole and the manipulator mounted on its body (Fig. 10). Two different cases will be considered for each leg. For the first case, we will consider that the body of the robot is fixed and the leg tip is free (the case of the transfer phase), and for the second case, we consider that the leg tip is fixed, and the movement will be performed by the body of the robot (the case of the support phase). We consider now the mechanism of the leg 1, for the situation in which the body of the robot is fixed (Fig. 16).
Solving the forward kinematics problem, we will get

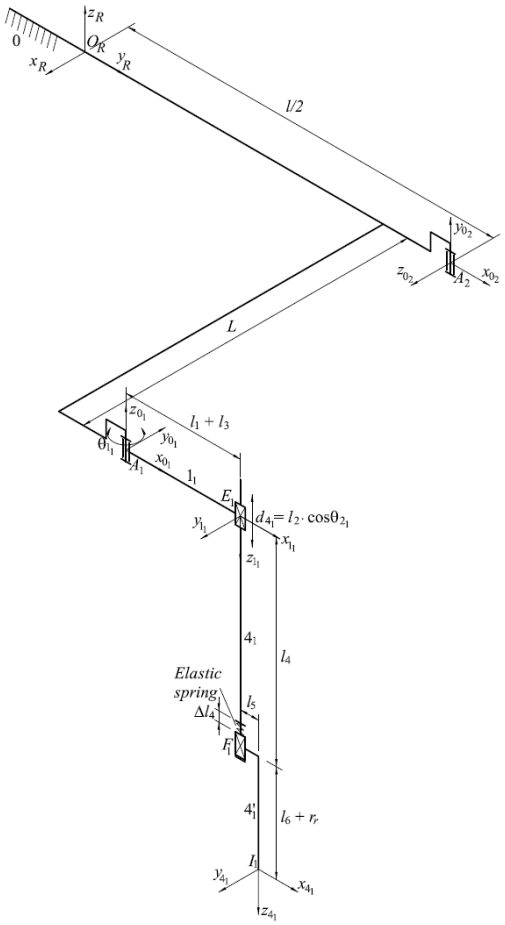

Fig. 16. The mechanism of the leg 1, mounted on the robot body, in case the robot body is fixed.

$$\begin{cases} {}^{O_R}x_{I_1} = -\left(l_1 + l_3 + l_5\right) \cdot \sin\theta_{1_1} + L \\ {}^{O_R}y_{I_1} = \left(l_1 + l_3 + l_5\right) \cdot \cos\theta_{1_1} + l/2 \\ {}^{O_R}z_{I_1} = -\left(d_{4_1} + l_4 + l_6 + r_r\right) = -\left(l_2 \cdot \cos\theta_{2_1} + l_4 + l_6 + r_r\right) \end{cases}, \quad (21)$$

where ${}^{O_R}x_{I_1}$, ${}^{O_R}y_{I_1}$, ${}^{O_R}z_{I_1}$ are the coordinates of the I_1 leg tip according to the origin O_R of the frame attached to the geometric center of the mobile robot body, and the inverse kinematics problem leads to

$$\theta_{1_1} = \operatorname{atan2}\left(\frac{L - {}^{O_R}x_{I_1}}{l_1 + l_3 + l_5}, \frac{{}^{O_R}y_{I_1} - l/2}{l_1 + l_3 + l_5}\right) \text{ and } \theta_{2_1} = \arccos\left[\frac{-\left({}^{O_R}z_{I_1} + l_4 + l_6 + r_2\right)}{l_2}\right] \quad (22)$$

We will now consider that the tip I_1 of the leg 1 is fixed, and we will determine the displacement of the O_R geometric center of the mobile robot according to I_1 (the case of the support phase), Fig. 17.

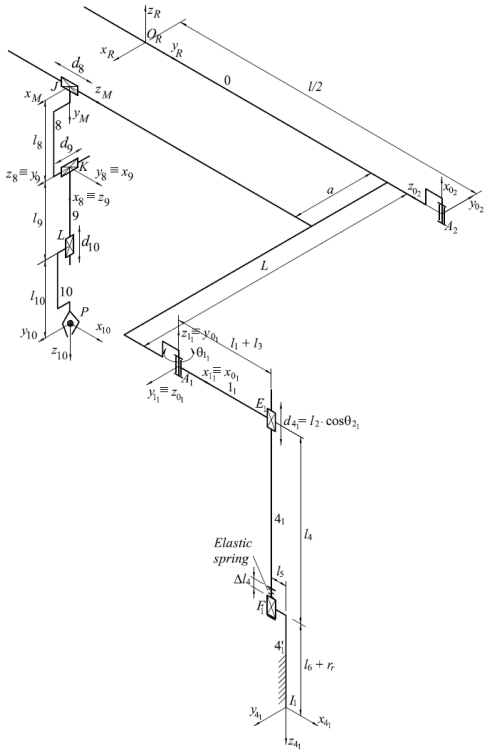

Fig. 17. The kinematic chain of the leg 1 and the manipulator, for the case when the leg tip is fixed.

Solving the forward kinematics problem, we will get

$$\begin{cases} {}^{I_1}x_{O_R} = -l/2 \cdot \cos\theta_{1_1} - L \cdot \sin\theta_{1_1} - \left(l_1 + l_3 + l_5\right) \\ {}^{I_1}y_{O_R} = l/2 \cdot \sin\theta_{1_1} - L \cdot \cos\theta_{1_1} \\ {}^{I_1}z_{O_R} = -\left(d_{4_1} + l_4 - \Delta l_4 + l_6 + r_r\right) = -\left(l_2 \cdot \cos\theta_{2_1} + l_4 - \Delta l_4 + l_6 + r_r\right) \end{cases}, \qquad (32)$$

where ${}^{I_1}x_{O_R}$, ${}^{I_1}y_{O_R}$, ${}^{I_1}z_{O_R}$ are the coordinates of the O_R robot center according to the I_1 leg tip, and the inverse kinematics problem leads to

$$\theta_{1_1} = \beta \pm \arccos\left[\frac{-{}^{I_1}y_{O_R}}{\sqrt{L^2 + \left(\frac{l}{2}\right)^2}}\right], \text{ with } \beta = \operatorname{atan2}\left[\frac{-\frac{l}{2}}{\sqrt{L^2 + \left(\frac{l}{2}\right)^2}}, \frac{L}{\sqrt{L^2 + \left(\frac{l}{2}\right)^2}}\right] \qquad (33)$$

$$\theta_{2_1} = \arccos\left[\frac{-\left({}^{I_1}z_{O_R} + l_4 - \Delta l_4 + l_6 + r_2\right)}{l_2}\right]. \tag{34}$$

Imposing the coordinates of the characteristic point *P* of the end manipulator effector, according to the geometric center of the robot body,

$$\begin{cases} {}^{O_R}x_P = a + d_9 \\ {}^{O_R}y_P = d_8 \\ {}^{O_R}z_P = -l_8 - l_9 - l_{10} - d_{10} \end{cases}, \tag{35}$$

the kinematic position parameters of the prismatic joints of this manipulator can also be determined,

$$d_8 = {}^{O_R}y_P\,,\ d_9 = {}^{O_R}x_P - a\,,\ d_{10} = -\left({}^{O_R}z_P - l_8 - l_9 - l_{10}\right). \tag{36}$$

5. Conclusions

One of the posible future solutions to eliminate the negative effect on the environment of the classical machineries is to use mobile robots for agricultural applications. For doing that, small groups of mobile robots have to work together and to interact with each other in order to inspect, to process or to harvest crops. These robots will have to work in a changing environment, in terms of terrain or road surfaces, the light of the ambient, animals, etc., aspects that will pose challenges for mobile robots. To facilitate the use of robots in agriculture, they must have a simple construction, be extremely reliable, flexible and, last but not least, cheap. These aspects have as effect new challenges for robot manufacturers to find technical solutions to meet the mentioned requirements. In this paper, a conceptual design and modeling of a mobile manipulator with hybrid locomotion, which may be used in agriculture for applications, such as tilling, seeding, weeding, etc, has beeen discussed. First, the agricultural applications, with examples, of mobile robots have been presented. Then, the locomotion systems used for these robots have been discussed. Based on some defined specifications and requirements, an agricultural robot with hybrid locomotion has been designed and realized. Then, the mathematical modeling of the robot, for the case of moving as a wheeled platform or as a walking machine was presented.

References

[1] Oliveira L.F.P., Moreira A.P., Silva M.F., *Advances in agriculture robotics: a state-of-the-art review and challenges ahead*, Robotics, **10**, 2, 2021, p. 52.
[2] Raussendorf. Fruit Robot. Available online: https://www.raussendorf.de/en/fruit-robot.html (accessed on 1 March 2023).

[3] Precision Makers. GREENBOT. Available online: https://www.precisionmakers.com/en/greenbot-2/ (accessed on 1 March 2023).
[4] Khan N., Medlock G., Graves S., Anwar S., *GPS Guided Autonomous Navigation of a small agricultural robot with automated fertilizing system*, SAE Technical Paper, SAE International: Warrendale PA, USA, 1, 2018, p. 1.
[5] Haibo L., Dong S., Zunmin L., Chuijie Y., *Study and experiment on a wheat precision seeding robot*, J. Robot., **1**, 2015, p. 1–9.
[6] Sukkarieh S., *Mobile on-farmdigital technology for smallholder farmers*, Proceedings of the 2017 Crawford Fund Annual Conference on Transforming Lives and Livelihoods: The Digital Revolution in Agriculture, Canberra, Australia, 7–8 August 2017, p. 92-100.
[7] Hassan M.U., Ullah M., Iqbal J., *Towards autonomy in agriculture: Design and prototyping of a robotic vehicle with seed selector*, Proceedings of the 2016 2nd International Conference on Robotics and Artificial Intelligence (ICRAI), Los Angeles, CA, USA, 20–22 April 2016, p. 37–44.
[8] Naio Tecnologies. OZ-Weeding, *Transportation and harvest assistance robot*. Available online: https://www.naio-technologies.com/wp-content/uploads/2019/04/brochure-OZ-ENGLISH-HD.pdf (accessed on 20 February 2023).
[9] Naio Tecnologies. Dino-Autonomous Mechanical Weeding Robot. Available online: https://www.naio-technologies.com/wp-content/uploads/2019/04/brochure-DINO-ENGLISH-HD.pdf (accessed on 20 February 2023).
[10] Naio Tecnologies. Ted—Multifunctional Straddling Vineyard Robot. Available online: https://www.naio-technologies.com/wp-content/uploads/2019/04/brochure-TED-ENGLISH-3.pdf (accessed on 20 February 202).3
[11] VITIROVER Solutions. VITIROVER—A Revolution in Soil Grassing Management. Available online: https://www.vitirover.fr/en-home (accessed on 23 February 2023).
[12] Franklin Robotics. Meet Tertill—A BetterWay toWeed. Available online: ttps://tertill.com/ (accessed on 23 February 2023).
[13] Choi K.H., Han S.K., Han S.H., Park K.H., Kim K.S., Kim S., *Morphology-based guidance line extraction for an autonomous weeding robot in paddy fields*, Comput. Electron. Agric., **113**, 2015, p. 266–274.
[14] Agrobot. The First Pre-Commercial Robotic Harvesters for Gently Harvest Strawberries. Available online: https://www.agrobot.com/e-series (accessed on 2 March 2023).
[15] Birrell S., Hughes J., Cai J.Y., Iida F., *A field-tested robotic harvesting system for iceberg lettuce*, J. Field Robot., **37**, 2020, p. 225–245.
[16] Ge Y., Xiong Y., Tenorio G.L., From P.J., *Fruit localization and environment perception for strawberry harvesting robots*, IEEE Access, **7**, 2019, p. 147642–147652.
[17] Bargoti S., Underwood J.P., *Image segmentation for fruit detection and yield estimation in apple orchards*, J. Field Robot., **34**, 2017, p. 1039–1060.
[18] Lopes C., Graça J., Sastre J., Reyes M., Guzman R., Braga R., Monteiro A., Pinto P., *Vineyard yield estimation by Vinbot Robot—preliminary results with the white variety viosinho*, Proceedings of the 11th International Terroir Congress, McMinnville, OR, USA, 10–14 July 2016.
[19] VineRobot. Available online: http://www.vinerobot.eu/ (accessed on 3 March 2023).
[20] Doroftei I., Morar C.A., Hagan M.G., *Design of a hybrid locomotion mobile manipulator for agricultural application*, I. Doroftei, B. Kiss, Y. Baudoin, Z. Taqvi, S. Keller Fuchter (Eds.). Proceeding of the 25th International Symposium on Measurement and Control in Robotics – ISMCR 2023, Iasi, Romania, 20-21 September 2023 (in press).
[21] Doroftei I., Morar C.A., Alaci S., Hagan M.G., *Kinematic design of a hybrid locomotion mobile manipulator for agricultural applications*, Acta Technica Napocensis-Series: Applied Mathematics, Mechanics, and Engineering, **65**(2S), 2022, p. 319-324.